Nasal administration of nanoencapsulated geraniol/ursodeoxycholic acid conjugate: design of a ~~possible~~ new approach ~~strategy~~ ~~against~~ for management of Parkinson's disease

Edilson Ribeiro de Oliveira Junior[a], Eleonora Truzzi[b], Luca Ferraro[c], Marco Fogagnolo[d], Barbara Pavan[e], Sarah Beggiato[c,f], Cecilia Rustichelli[b], Eleonora Maretti[b], Eliana Martins Lima[a], Eliana Leo[b,*], Alessandro Dalpiaz[d,*]

[a] *School of Pharmacy, Laboratory of Pharmaceutical Technology – FamaTec, Federal University of Goiás, Rua 240, esquina com 5a Avenida, s/n, Setor Universitário, Goiânia, CEP 74605-170, Brazil*

[b] *Department of Life Sciences, University of Modena and Reggio Emilia, Via Campi 103, I-41125 Modena, Italy*

[c] *Department of Chemical and Pharmaceutical Sciences, University of Ferrara, Via Fossato di Mortara 19, I-44121 Ferrara, Italy*

[d] *Department of Life Sciences and Biotechnology, University of Ferrara and LTTA Center, Via L. Borsari 46, I-44121 Ferrara, Italy*

[e] *Department of Biomedical and Specialist Surgical Sciences, University of Ferrara, Via L. Borsari 46, 44121 Ferrara, Italy*

[f] *Department of Medical, Oral and Biotechnological Sciences, University of Chieti-Pescara, Italy*

* Corresponding author.

E-mail address: dla@unife.it (A. Dalpiaz); eliana.leo@unimore.it (E. Leo).

ABSTRACT

The combined use of different therapeutic agents in the treatment of neurodegenerative disorders is a promising strategy to halt the disease progression. In this context, we aimed to combine the anti-inflammatory properties of geraniol (GER) with the mitochondrial rescue effects of ursodeoxycholic acid (UDCA) in a newly-synthesized prodrug, GER-UDCA, a potential candidate against Parkinson's disease (PD). GER-UDCA was successfully synthetized and characterized *in vitro* for its ability to release the active compounds in physiological environments. Because of its very poor solubility, GER-UDCA was entrapped into both lipid (SLNs) and polymeric (NPs) nanoparticles in order to explore nose-to-brain pathway towards brain targeting. Both GER-UDCA nanocarriers displayed size below 200 nm, negative zeta potential and the ability to increase the aqueous dissolution rate of the prodrug. As SLNs exhibited the higher GER-UDCA dissolution rate, this formulation was selected for the *in vivo* GER-UDCA brain targeting experiments. The nasal administration of GER-UDCA–SLNs (1 mg/kg of GER-UDCA) allowed to detect the prodrug in rat cerebrospinal fluid (concentration range = 1.1 to 4.65 µg/mL, 30-150 min after the administration), but not in the bloodstream, thus suggesting the direct nose to brain delivery of the prodrug. Finally, histopathological evaluation demonstrated that, in contrast to the pure GER, nasal administration of GER-UDCA-SLNs did not damage the structural integrity of the nasal mucosa. In conclusion, the present data suggest that GER-UDCA-SLNs could provide an effective and non-invasive approach to boost the access of GER and UDCA to the brain with low dosages.

Keywords ***MAX 6:*** Geraniol, ursodeoxycholic acid, ~~conjugation,~~ ~~hydrolysis,~~ prodrug, solid lipid nanoparticles, nasal administration, ~~brain uptake~~ Parkinson's disease

1. Introduction

Parkinson's disease (PD), firstly described in 1817, is a neurodegenerative disorder mainly characterized by the degeneration of dopaminergic neurons in the *substantia nigra* (SN), which leads to several severe symptoms [1]. In spite of numerous therapies aimed to attenuate the motor symptoms caused by dopamine deficiency, none of them has been able to prevent or arrest the progression of PD so far. Among the well-established key mechanisms of PD pathogenesis, both neuroinflammation and mitochondrial dysfunction in dopaminergic neurons are, currently, considered the main causes leading to the progression of the disease. In neuroinflammation, the long-term activation of the microglia, the major resident immune cells in the brain, drives to an uncontrolled production of pro-inflammatory cytokines and reactive oxygen species (ROS), accelerating neuron degeneration [2,3]. Mitochondrial dysfunction in dopaminergic neurons is mainly characterized by the generation of ROS, cytochrome-c release, ATP depletion, decrease in mitochondrial complex I enzyme activity, and caspase 3 activation. The impaired mitochondrial function leads to the activation of death signaling pathways and to deficit in neuron homeostasis [4-6]. Therefore, a therapeutic approach aimed at reducing both neuroinflammation and mitochondrial dysfunction may prove to be effective in slowing/arresting the progression of the disease.

Natural compounds are a potential source for novel therapeutic agents. As an example, geraniol (GER) is a monoterpene present in several essential oils extracted from aromatic plants, which exhibits a wide spectrum of pharmacological activities, such as neuroprotective, anti-inflammatory and antioxidant properties [7]. Furthermore, Rekha & Selvakumar demonstrated that orally administered GER promotes the survival of dopaminergic neurons. ~~The mechanisms shown included enhancing the production of antioxidant enzymes, reducing the expression of apoptotic markers and increasing the production of neurotrophic factors [8].~~ The suggested mechanisms included an enhancement of the production of antioxidant enzymes, a reduction of the apoptotic marker expression and an increasing in the production of neurotrophic factors [8]. In addition, beneficial effects of GER in PD animal models have been further reported in the literature [7, 9-10]. The combination of the abovementioned properties, along with its low toxicity potential [11], makes GER a potential candidate for the treatment of PD.

However, the short half-life of GER in the bloodstream could limit its use in long term therapies through the conventional administration routes [7,12].

Recently, the secondary bile acid, ursodeoxycholic acid (UDCA), commonly used for the treatment of liver disease, was proven effective in rescuing mitochondrial function in parkinsonian patients and it is now in phase II of a clinical trial in PD patients [13-14]. UDCA showed the ability to interact with the glucocorticoid receptor with increased phosphorylation of the protein Akt, exerting a protective effect against mitochondria-dependent programmed cell death [15]. Moreover, Parry *et al.* documented the safety and tolerability of UDCA, at doses up to 50 mg/kg per day, in patients with motor neuron disease [16]. UDCA has been clinically used for the treatment of primary biliary cirrhosis for more than 30 years, and its clinical pharmacokinetics is well-established [17,18].

Based on the above reported background, in the present work we synthetized the ester conjugate of GER with UDCA (GER-UDCA, Fig. 1). We considered this conjugate as a prodrug candidate, combining the pharmacological properties of GER and UDCA for the development of a new therapeutic strategy against PD progression/development. However, the resulting compound remained nearly insoluble in water and presented a highly viscous and sticky physical aspect. As such, we prepared both lipid and polymer-based nanoparticles as GER-UDCA delivery systems.

Nevertheless, reaching therapeutic levels in the central nervous system (CNS) is a challenge for most drugs. In light of that, we chose the intranasal route of administration to explore the nose-to-brain delivery of GER-UDCA. In fact, the olfactory region is known to potentially induce the direct transport of drugs or prodrugs into the CNS [19-21]. We also hypothesized that this pathway might contribute to overcome low CNS bioavailability following oral administration.

Specifically, in the present study GER-UDCA prodrug was firstly synthesized and, after the characterization of its aptitude to be hydrolyzed in physiologic environments, it was entrapped in nanoparticles and intranasally administered ~~via nose to brain~~ to rats.

2. Materials and methods

2.1. Materials

UDCA was kindly supplied by ICE Srl (RE, Italy) and used without purification. GER (98%), carbazole, *N*-ethyl-*N'*-(3-dimethylaminopropyl) carbodiimide hydrochloride (EDCI·HCl), HPLC-grade methanol, acetonitrile, ethyl acetate (EtOAc); Span 85, Tween 80, PLGA 75:25, Pluronic-F127 and sodium taurocholate hydrate 97% were acquired from Sigma-Aldrich (Milan, Italy). Compritol ATO 888 was a kind gift from Gattefossè (Saint Priest, France). All other chemicals were of analytical grade.

2.2. ~~Synthesis~~ Analytical assays

Thin layer chromatography (TLC) was performed on pre-coated silica gel glass plates 60F254 (thickness 0.25 mm, Merck). Reagents and compounds were detected under short wavelength UV light and by heating after spraying with a 5% phosphomolybdic acid solution. Silica gel (Fluka, Kieselgel 60, 70−230 mesh) was used for preparative column chromatography. ^{1}H and ^{13}C-NMR spectra were recorded on 400 MHz spectrometers in $CDCl_3$ at room temperature. Chemical shifts are given in parts per million (ppm); J values are given in hertz (Hz). All spectra were internally referenced to the appropriate residual undeuterated solvent. Mass spectra were recorded using a LCQ Duo (ThermoQuest, San Jose, CA, USA), equipped with an electrospray ionization (ESI) source. IR spectra were recorded on a Perkin-Elmer FT-IR Paragon 500.

2.3. Synthesis of GER-UDCA conjugate.

A solution of UDCA (1.50 g, 3.82 mmol), GER (0.65 g, 4.20 mmol) and 4-dimethylaminopyridine (DMAP) (0.46 g, 3.82 mmol) in dry DMF (8 mL) was treated at 0°C with EDCI·HCl (0.80 g, 4.20 mmol). The reaction mixture was stirred at 0°C for 1 h then at room temperature monitored by TLC (cyclohexane/EtOAC 40:60). After 20 h the mixture was evaporated under vacuum to dryness, then EtOAc (50 mL) was added. The organic layer was washed with 5% aqueous HCl (30 mL), saturated aqueous $NaHCO_3$ (40 mL) and brine (40 mL), then dried (Na_2SO_4), filtered and concentrated in

vacuo. Chromatography on silica gel (cyclohexane/EtOAc mixture 40:60) provided product **1** (1,67 g, 83%) as a sticky solid.

^{1}H-NMR (400 MHz, $CDCl_3$): δ 5.32 (t, J = 6.8 Hz, 1H), 5.07 (br, 1H), 4.58 (d, J = 6.8 Hz , 2H), 3,57 (br, 2H), 2.40-2.14 (m, 2H), 2.15-1,0 (m, 39 H), 0.93 (s, 3H), 0.91 (d, J = 6,4 Hz, 3H), 0.66 (s, 3H).

^{13}C{1H}-NMR (101 MHz, $CDCl_3$): δ 174.28, 142.14, 131.80, 123.73, 118.33, 71.42, 71.35, 61.21, 55.68, 54.88, 46.53, 43.74, 42.41, 40.10, 39.52, 39.14, 37.27, 36.79, 35.23, 34.90, 34.05, 31.32, 31.01, 30.31, 28.58, 26.88, 26.28, 25.68, 23.37, 21.14, 18.37, 17.69, 16.47, 12.11.

FT-IR (neat, cm^{-1}): νmax 3345, 2927, 1733, 1671, 1161. ESI-MS: m/z 551.33 $(M + Na)^+$

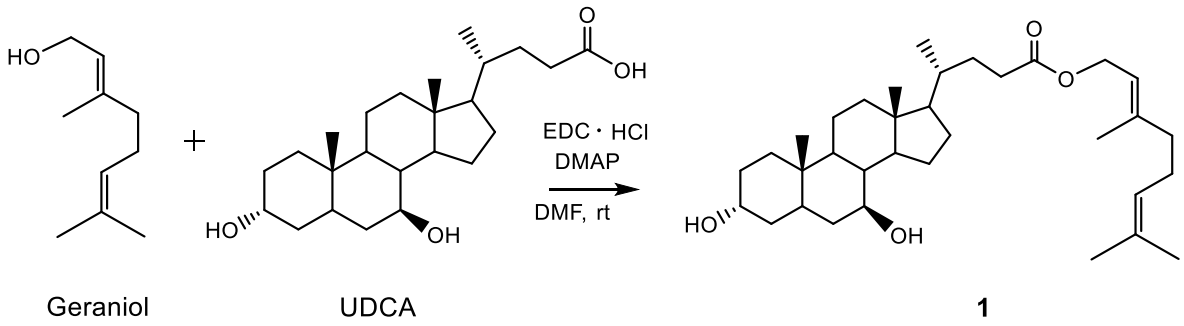

Fig. 1. Synthesis of the conjugate GER-UDCA (1)

2.4. HPLC analysis

The quantification of the GER-UDCA prodrug and its hydrolysis product, GER, was performed by HPLC-UV. Please see Supplementary Methods for a detailed description of the analytical procedures.

~~The chromatographic apparatus consisted of a modular system (model LC-10 AD VD pump and model SPD-10A VP variable wavelength UV-vis detector; Shimadzu, Kyoto, Japan) and an injection valve with 20 µL sample loop (model 7725; Rheodyne, IDEX, Torrance, CA, USA). Separations were performed at room temperature on a 5 µm Hypersil BDS C-18 column (150 mm × 4.6 mm i.d.; Alltech Italia Srl, Milan, Italy), equipped with a guard column packed with the same Hypersil~~

material. Data acquisition and processing were accomplished with a personal computer using CLASS-VP Software, version 7.2.1 (Shimadzu Italia, Milan, Italy). The detector was set at 210 nm. The HPLC assay of GER alone was isocratically performed with a mobile phase constituted by a mixture of CH_3CN and H_2O 50:50 (v/v). The flow rate was 1 mL/min and the retention time 4.7 min. The HPLC assay of GER-UDCA alone was isocratically performed with a mobile phase constituted by a mixture of CH_3CN and H_2O 90:10 (v/v). The flow rate was 1 mL/min and the retention time 5.5 min. The isocratic conditions were used for the evaluation of GER loaded in the nanoparticles and GER-UDCA solubility, its loading and release from nanoparticles (see below). The chromatographic precision for GER and GER-UDCA dissolved in a water-acetonitrile mixture (50:50 v/v) was evaluated by repeated analysis ($n = 6$) of the same sample (100 μM) and it is represented by the relative standard deviation (RSD) values of 0.91% and 0.89%, respectively, referred to peak areas. The calibration curves of peak areas versus concentration were generated in the range 1 to 500 μM for GER and GER-UDCA dissolved in a mixture of aqueous phase and acetonitrile (50:50 v/v ratio). The calibration of GER and GER-UDCA alone were also performed in pure acetonitrile (for GER or GER-UDCA loading studies). Moreover, the calibration of GER-UDCA was performed in 50 mM Tris-HCl buffer (pH 7.4) mixed to 10% methanol (for kinetic studies) and in water with 5 mM sodium dodecyl sulfate (SDS, for release studies). All the calibration curves of GER and GER-UDCA were linear ($n = 10$, $r > 0.995$, $P < 0,0001$).

In order to simultaneously quantify GER and GER-UDCA in blood or homogenate extracts, the mobile phase consisted of a mixture of water and acetonitrile regulated by a gradient profile programmed as follows: isocratic elution with 40% (v/v) CH_3CN in H_2O for 11 min; then a 4 min linear gradient to 90% (v/v) CH_3CN in H_2O; the mobile phase composition was finally maintained at 90% CH_3CN for 8 min. After each cycle the column was conditioned with 40% (v/v) CH_3CN in H_2O for 10 min. The flow rate was 1 mL/min. Carbazole was used as internal standard for the analysis of rat blood and liver or brain homogenate extracts (see below). The retention times for GER, carbazole and GER-UDCA were 10.5, 14.9 and 21.3 min, respectively.

The precision evaluation and calibration procedures following the extraction of the analytes from homogenates and whole blood were performed in the presence of the

~~internal standard (carbazole) and are described in the appropriate sections (see 2.9. and 2.15.)~~

~~*2.5. Water solubility of GER-UDCA*~~

~~For determining the solubility of GER-UDCA, an excess amount of the naked compound (2 mg/mL) was added to 5 mL of water and left to equilibrate at room temperature under continuous stirring for 36 h. After centrifugation at 14,000 g for 15 min, a supernatant aliquot was mixed with acetonitrile (50:50 v/v ratio), then 10 µl of the mixture was injected into the HPLC system for GER-UDCA quantification. The experiments were performed in triplicate.~~

~~*2.6. GER and GER-UDCA stock solutions.*~~

~~Stock solutions of $5{\cdot}10^{-2}$ M GER and GER-UDCA in DMSO were prepared and stored at -20 °C until their use for kinetic studies.~~

2.5. Kinetic analysis of GER-UDCA in Tris-HCl buffer.

The conjugate GER-UDCA was incubated at 37 °C in 50 mM Tris-HCl buffer (pH 7.4) mixed to 10% methanol (v/v, final concentration) in order to increase the GER-UDCA solubility and to obtain its 50 µM final concentration. In particular, $5{\cdot}10^{-2}$ M stock solution in DMSO was diluted 1:100 in methanol, then 5.4 mL of Tris-HCl 50 µM were spiked with 600 µL of the 500 µM solution of GER-UDCA in methanol. At regular time intervals 200 µL of samples were withdrawn and 10 µL aliquots were immediately injected into the HPLC apparatus in order to quantify the GER and GER-UDCA amounts. All the values were obtained as the mean of three independent experiments.

2.6. Preparation of rat brain and liver homogenates

Rat brain and liver homogenates were prepared as Tris-HCl water suspension. For further details, please see Supplementary Methods

~~Brains of male Sprague-Dawley rats (Charles-River, Milan, Italy) were immediately isolated after their decapitation and homogenized in 5 volumes (w/v) of Tris-HCl (50 mM, pH 7.4, 4 °C) with an ultra-Turrax (IKA-Werke GmbH & Co. KG, Staufen, Germany) using 3 × 15 s bursts. The supernatant obtained after centrifugation (3,000 x g for 15 min at 4 °C) was decanted off and stored at −80°C before its use for kinetic studies. The total protein concentration in the tissue homogenate was determined using the Lowry procedure [22] and resulted as 7.2 ± 0.4 µg protein/µL.~~

~~The livers of male Sprague-Dawley rats were immediately isolated after their decapitation, washed with ice cold saline solution and homogenized in 4 volumes (w/v) of Tris-HCl (50 mM, pH 7.4, 4 °C) with the use of a Potter-Elvehjem apparatus. The supernatant obtained after centrifugation (2,000 g for 10 min at 4 °C) was decanted off and stored at -80 °C before its use for kinetic studies. The total protein concentration in the tissue homogenate resulted as 29.4 ± 1.1 µg protein/µL.~~

2.7. Kinetic analysis of GER and GER-UDCA in rat brain or rat liver homogenates

GER or the conjugate GER-UDCA were singularly incubated at 37 °C in 3 mL of rat brain or rat liver homogenates, resulting in a final concentration of 500 µM obtained by adding 10 µL of $5 \cdot 10^{-2}$ M stock solution in DMSO for each milliliter incubated. At regular time intervals, 100 µL of samples were withdrawn and immediately quenched in 200 µL of ethanol (4° C); 100 µL of internal standard (100 µM carbazole dissolved in ethanol) was then added. After centrifugation at 13,000 x g for 10 min, 300 µL aliquots of supernatant were reduced to dryness under a nitrogen stream, then 150 µL of a water and acetonitrile mixture (50:50 v/v) was added, and, after centrifugation, 10 µL was injected into the HPLC system. In order to evaluate the potential influence of unloaded nanoparticles on GER-UDCA hydrolysis, the same procedure was adopted for the analysis of rat liver homogenate samples containing the free prodrug in combination with unloaded NPs using the same amounts employed for the loaded ones. The only difference was the addition of 50 µL of dichloromethane to the withdrawn samples before the extraction procedure. All the values were obtained as the mean of three independent incubation experiments.

Recovery experiments were performed by comparing the peak areas extracted from brain or liver homogenate test samples (100 µM) at 4 °C with those obtained by injection of an equivalent concentration of the analytes dissolved in water-acetonitrile mixture (50:50 v/v). The average recoveries ± SD were 56.7 ± 2.3% for the GER extracted from rat brain homogenate; 38 ± 1.9% for the GER extracted from rat liver homogenate; 69.3 ± 3.8% for the conjugate GER-UDCA extracted from rat brain homogenate; 86.2 ± 4.7% for the conjugate GER-UDCA extracted from rat liver homogenate. The concentrations of GER and GER-UDCA were therefore referred to as peak area ratio with respect to their internal standard carbazole. The precision of the method based on peak area ratio was represented by RSD values in the different homogenates ranging between 1.33% and 1.41% for 100 µM GER or between 1.18% and 1.21% for 100 µM GER-UDCA. For all compounds analyzed, the calibration curves were constructed by using ten different concentrations in homogenates at 4 °C ranging from 5 to 500 µM and expressed as peak area ratios of the compounds and the internal standard *versus* concentration. The calibration curves were linear ($n = 10$, $r \geq 0.995$, $P < 0.0001$).

A preliminary analysis performed on blank rat liver homogenate samples showed that their components did not interfere with the GER, GER-UDCA, and carbazole retention times.

The half-life value of the conjugate GER-UDCA incubated in rat liver homogenate was calculated from an exponential decay plot of its concentrations versus incubation time, using the computer program GraphPad Prism (GraphPad, San Diego, CA). The same software was used for the linear regression of the corresponding semilogarithmic plot. The quality of the fits was determined by evaluating the correlation coefficients (r) and P values.

2.8. Preparation of GER and GER-UDCA-loaded nanoparticles

Solid lipid nanoparticles (SLNs) were prepared by emulsification/evaporation solvent method. Firstly, compritol ATO 888 (120 mg), Span 85 (40 mg) and 30 mg of GER-UDCA were dissolved in 3 mL of chloroform. This organic phase was dropped

into 5 mL of aqueous phase (Tween 80 1% + Taurocholate sodium salt 1%, w/v) and homogenized by UltraTurrax (Ika-euroturrax T 25 basic, IkaLabortechnik, Staufen, Germany) at 24,000 rpm for 5 min. The O/W emulsion was poured quickly into 15 mL of the aqueous phase and sonicated at 20W for 3 min in an ice bath. The resulting suspension was maintained in magnetic stirring for 2 h to allow the solvent evaporation. Finally, SLNs were purified by dialysis (12,000 – 14,000 Da cut-off) for 30 min and freeze-dried for 48 h (Lio 5P, Cinquepascal, Milan, Italy).

PLGA nanoparticles (NPs) were obtained by nanoprecipitation method. Briefly, PLGA (100 mg) and GER-UDCA (30 mg) were dissolved in a solvent mixture (4 mL acetonitrile + 2 mL methanol). Then, the organic phase was added into 30 mL of aqueous phase containing 0.1% w/v of Pluronic-127 under magnetic stirring. The formulation was kept under magnetic stirring overnight to complete the elimination of organic solvents. NPs were purified 3 times by centrifugation (5,000 x g) (Rotina 380R, Hettich, Germany) in 100 kDa MWCO Vivaspin (Sartorius, Goettingen, Germany) columns and freeze-dried for 48 h (Lio 5P).

For comparison, in order to evaluate the possibility to encapsulate in nanoparticles only GER in liquid form, GER-loaded SLNs and NPs were prepared according to the same protocol previously described. For other procedures adopted in the preparation of GER-loaded nanoparticles see Supplementary Materials.

2.9. Particle size, zeta potential and morphological analysis

Particle size, polydispersity index (PDI) and zeta-potential were measured by Photon Correlation Spectroscopy (PCS) (Zetasizer version 6.12, Malvern Instruments, Worcs, U.K. equipped with a 4 mW HeNe laser (633 nm) and a DTS software (Version 5.0)) at 25°C. Freshly prepared formulations were diluted in purified deionized water (1:5) and the analysis was performed in triplicate, each measurement was averaged over at least 12 runs.

SLNs morphology was determined by Atomic Force Microscopy (AFM) (Park Autoprobe Atomic Force Microscope, Park Instruments, Sunnyvale, CA, USA) at room temperature (25 °C), operating in non-contact mode, with resonance frequencies from 100 to 200 kHz. SLNs suspension was deposited onto a small mica disk with a diameter of 1 cm. Topographical AFM images was processed using Gwyddion (2.5 version) software. NPs morphology were observed by field-emission gun scanning electron

microscopy (SEM-FEG, Nova NanoSEM 450, Fei, Eindhoven, The Netherlands) using both Scanning Electron Microscopy (SEM) and Scanning Transmission Electron Microscopy mode (STEM). NPs suspension was dropped on aluminium stub or carbon/copper grids for SEM-FEI and STEM, respectively, and after drying, coated with carbon under vacuum conditions (Carbon Coater, Balzers CED-010, Oerlikon Balzers, Balzers, Liechtenstein).

2.10. GER and GER-UDCA loading and entrapment efficiency

Formulations (2 mg) were dissolved in acetonitrile (2 mL) heated at 50 °C for 15 min. Then, samples were vortexed for 5 min and centrifuged at 14,000 g for 10 min. The supernatant was re-centrifuged, then 10 µL was injected into HPLC system for GER-UDCA quantification. All experiments were performed in triplicate. The drug loading (DL %) and drug entrapment efficiency (EE %) were calculated according to the following equations:

$$EE\% = \frac{Amount\ of\ prodrug\ in\ purified\ sample}{Total\ amount\ of prodrug\ used}\ x\ 100$$

$$DL\% = \frac{Amount\ of\ incorporated\ prodrug}{Total\ mass\ of\ freeze-dried\ sample}\ x\ 100$$

2.11. In vitro drug release

In vitro release profiles of GER-UDCA from nanocarriers were evaluated by ultracentrifugation separation technique. 0.5 mg of GER-UDCA or equivalent pro-drug amount loaded in freeze-dried nanoparticles were suspended into 75 mL of water with SDS 5 mM at 37 °C under magnetic stirring (100 rmp). At predefined time points (0.25, 0.5, 1, 1.5, 2, 4, 6 and 8h), 150 µL of sample were withdrawn and replaced by fresh release medium. The samples were centrifuged at 4°C in order to prevent further drug release, at 24,000 x g (Rotina 380R) for 20 min and the supernatant analyzed by HPLC, as described above. ~~The centrifuge temperature was 4°C in order to prevent further release of drug.~~ All experiments were performed in triplicate.

2.12. Hydrolysis studies of free and encapsulated GER-UDCA in rat liver homogenates

Stability studies on the nanoencapsulated GER-UDCA were performed by spiking the rat liver homogenate (3 mL) at 37 °C with loaded NPs or SLNs, resulting in a final concentration of about 500 µM for GER-UDCA. Because the loaded nanoparticles were suspended in the medium, it was difficult to withdraw several homogeneous samples, and consequently stability was assessed by a single sampling after 120 min incubation. Dichloromethane (1 mL) was added, and 250 µL was withdrawn from the samples and quenched in 400 µL of ice-cold ethanol added with 200 µL of 100 µM carbazole dissolved in ethanol as internal standard. After 10 min of centrifugation at 13,000 x g, 600 µL aliquots were reduced to dryness under a nitrogen stream. The obtained residue was re-dissolved in 300 µL of the water-acetonitrile mixture (50:50 v/v) and, after centrifugation, 10 µL was injected into the HPLC system for GER and GER-UDCA detection. All the values obtained are the mean of three independent experiments.

2.13. In Vivo GER and GER-UDCA ~~nasal~~ administration ~~and quantification~~.

2.13.1. Intravenous infusion of GER-UDCA

Male Sprague-Dawley rats (200-250 g) fasted for 24 h were anesthetized during the experimental period and received a femoral intravenous infusion of 1 mg/mL of GER-UDCA dispersed in a medium constituted by 20% (v/v) DMSO and 80% (v/v) physiologic solution in the presence of 0.82 mg/mL sodium taurocholate, at a rate of 0.1 mL/min for 5 min. At the end of the infusion and at fixed time points, blood samples (100 mL) were collected and CSF samples (50 µL) were withdrawn. The blood samples (n = 4) were hemolyzed immediately after their collection with 500 µL of ice-cold water, and then 50 µL of 10% sulfosalicylic acid and 50 µL of internal standard (100 µM carbazole dissolved in a water-methanol mixture 50:50 v/v) was added. The samples were extracted twice with 1 mL of water saturated ethyl acetate, and, after centrifugation, the organic layer was reduced to dryness under a mild nitrogen stream at room temperature. Then, 150 µL of a water-acetonitrile mixture (50:50 v/v) was added, and, after centrifugation, 10 µL was injected into the HPLC system for GER and GER-UDCA detection. Recovery experiments were performed comparing the peak areas

extracted from blood test samples (10 µM) at 4 °C (n = 6) with those obtained by injection of an equivalent concentration of the analytes dissolved in water-acetonitrile mixture (50:50 v/v). The average recoveries ± SD were 60.9 ± 2.8% and 74.6 ± 4.0% for GER and the conjugate GER-UDCA, respectively. Their concentrations were therefore referred to as peak area ratio with respect to the internal standard carbazole. The precision of the method based on peak area ratio was represented by RSD values of 1.38% and 1.20% for GER and the conjugate GER-UDCA, respectively. The calibration curves referred to these compounds were constructed by using eight different concentrations in whole blood at 4 °C ranging from 2 to 40 µM (0.30 to 6.2 µg/mL) for GER and from 5 to 150 µM (2.64 to 79.2 µg/mL) for GER-UDCA and appeared linear ($n = 8$, $r \geq 0.995$, $P < 0.0001$). The limit of detection (LOD) and limit of quantification (LOQ) values of GER-UDCA in rat whole blood were 0.8 µg/mL (8 ng/injection, signal-to-nose ratio = 3:1) and 2.6 µg/mL (26 ng injection, signal to nose ratio = 10:1), respectively. The LOD and LOQ values of geraniol in rat whole blood were 0.09 µg/mL (0.9 ng injection, signal-to-nose ratio = 3:1) and 0.30 µg/mL (3.0 ng injection, signal-to-nose ratio = 10:1), respectively.

The CSF was withdrawn using the cysternal puncture method described by van den Berg et al. [22], which requires a single needle stick and allows the collection of serials (40-50 µL) CSF samples that are virtually blood-free [21]. A total volume of about a maximum of 150 µL of CSF/rat (*i.e.* three 50 µL samples/rat) was collected during the experimental session, choosing the time points (n = 4-6, taking into account a maximum of three collections for rat) in order to allow the restoring of the CSF physiological volume. The CSF samples (10 µL) were immediately injected into the HPLC system for GER and GER-UDCA detection. For CSF simulation, standard aliquots of balanced solution (PBS Dulbecco's without calcium and magnesium) in the presence of 0.45 mg/mL BSA were used [23,24]. In this case, the chromatographic precision was evaluated by repeated analysis (n = 6) of the same sample solution containing 5 µM of GER (0,77 µg/mL) or GER-UDCA (2.65 µg/mL) and it is represented by the RSD values of 1.18% or 1.02%, respectively, referred to peak areas. The calibration curves of peak areas versus concentration in CSF simulation fluid of the analytes were generated in the range 1 to 300 µM for GER (0.15 to 46.5 µg/mL) and 1 to 40 µM for GER-UDCA (0.53 to 20.1 µg/mL), appearing linear ($n = 8$, $r \geq 0.994$, $P < 0.0001$). The limit of detection (LOD) and limit of quantification (LOQ) values of GER-

UDCA in CSF simulation fluid were 0.16 µg/mL (16 ng/injection, signal-to-nose ratio = 3:1) and 0.53 µg/mL (53 ng injection, signal to nose ratio = 10:1), respectively. The LOD and LOQ values of GER in CSF simulation fluid were 0.05 µg/mL (0.5 ng injection, signal-to-nose ratio = 3:1) and 0.15 µg/mL (1.5 ng injection, signal-to-nose ratio = 10:1), respectively.

A preliminary analysis performed on blank CSF and blood samples showed that their components did not interfere with the GER, GER-UDCA, and carbazole retention times.

A further group of rats (n = 4) received also a femoral intravenous infusion of 5 mg/mL of GER-UDCA dispersed in a medium constituted by 20% (v/v) DMSO and 80% (v/v) physiologic solution in the presence of 0.82 mg/mL sodium taurocholate, at a rate of 0.1 mL/min for 5 min. At the end of the infusion and at fixed time points, blood samples (100 mL) were collected and analyzed as above described for GER and GER-UDCA detection.

The in vivo half-life ($t_{1/2}$) of GER-UDCA in the bloodstream of rats was calculated by nonlinear regression (exponential decay) of concentration values in the time range within 3 h after infusion and confirmed by linear regression of the log concentration values versus time (semilogarithmic plot). The area under concentration curve of GER-UDCA in bloodstream or CSF of rats (AUC, $\mu g \cdot mL^{-1} \cdot$ min) was calculated by the trapezoidal method. The clearance (CL) and distribution volume (Vd) values were calculated according to the non-compartmental model as the ratios "dose/AUC" and "CL/k_{el}", respectively, where k_{el} is the elimination constant obtained by the slope of semilogarithmic plot.

All the calculations were performed by using Graph Pad Prism software, version 7 (GraphPad Software Incorporated, La Jolla, CA, USA).

2.13.2. Nasal administration of GER and GER-UDCA

Adult male Sprague-Dawley rats (200-250 g body weight) fasted for 24 h, anesthetized and laid on their backs, received by nasal route about 1 mg of GER (4 mg/kg) or about 500 µg of GER-UDCA (2 mg/kg). In particular, 55 µl of GER emulsified (10 mg/mL, corresponding to 11.4 µL/mL) in a mixture of glycerol and

water 60:40 (v/v), or 55 µl of an aqueous suspension containing an amount of loaded SLNs corresponding to about 250 µg of GER-UDCA was introduced in each nostril of rats. The nasal administrations were performed using a semiautomatic pipet which was attached to a short polyethylene tubing. The tubing was inserted approximately 0.6–0.7 cm into each nostril. After the administration, blood (100 µL) and CSF samples (50 µL) were serially collected at fixed time points from each rat and analyzed as above described.

All *in vivo* experiments were performed in accordance with the European Communities Council Directive of September 2010 (2010/63/EU). Any effort has been done to reduce the number of the animals and their suffering.

2.14. Histopathological examinations of nasal mucosa

The short-term effect of GER and GER-UDCA-SLNs on the structural integrity of nasal mucosa was evaluated on adult male Wistar rats weighing 250-300 g (obtained from the Central Animal Facility at Federal University of Goiás). Animals were acclimatized for a week prior to the beginning of experiments and kept under 12:12 h light-dark cycles at 25°C ± 1°C with food and water ad libitum. GER, GER-UDCA-SLNs, PBS 7.4 (as negative control) and pure isopropyl alcohol (as positive control) were administered intranasally in rats (n=3). GER and GER-UDCA formulations were the same used for the uptake studies in CSF (section 2.13.2). Nasal administration was performed by introducing 55 µl of the sample in each nostril using a semiautomatic pipet, by inserting 0.6-0.7 cm of the attached polyethylene tubing into the nostrils. After 2h from the administration, the nasal mucosa was carefully removed. Tissues were washed in PBS, fixed in 10% v/v of formalin solution overnight and paraffin-embedded. Finally, slide samples (5 µm) were prepared using a microtome, stained with hematoxylin-eosin and observed under optical microscope (40x) to evaluate the mucosa integrity.

In vivo experiments were approved by the Federal University of Goiás (UFG) Animal Research Ethics Committee (protocol 38/18). Experimental protocols followed the principles for laboratory animal care and the Brazilian legislation (Law 11,794, October 8, 2008).

2.15. Statistical analysis

Statistical comparisons between percentage values of GER-UDCA and GER obtained by incubation of the free or encapsulated prodrug in liver homogenates were performed by one-way ANOVA followed by Dunnet post-test. Statistical comparison of the nanoparticle size was performed by one-way ANOVA test considering $p < 0.05$ statistically significant. Statistical comparison AUC test was performed by Student's test. $P < 0.05$ was considered statistically significant. The calculations were performed by using the computer program Graph Pad Prism.

3. Results

3.1. Synthesis of GER-UDCA prodrug.

The GER-UDCA prodrug 1 was obtained as sticky solid in 83% yield and ≥ 98% purity as determined by their ^{1}H-NMR analysis after column chromatography. The molecular weight, ^{1}H-NMR, ^{13}C-NMR and IR spectra of prodrug were in agreement with those required by its structure. No by-products of UDCA self-esterification have been observed because the secondary OH groups of the steroid, due to the steric hindrance, are much less reactive than the primary hydroxyl group of GER. Instead, some unreacted starting materials were present in the crude reaction mixture.

3.2. Hydrolysis and solubility studies of GER-UDCA

A first step of the present work was the evaluation of the potential hydrolysis pattern of the GER-UDCA conjugate in different media such as Tris-HCl buffer, rat brain and liver homogenates. The second step was the nasal administration of GER-UDCA loaded in nanoparticulate systems and its detection in CSF and whole blood of rats. Toward these aims it was firstly necessary to detect and quantify not only the

conjugate, but also GER, obtainable by the potential hydrolysis of the prodrug in all incubation media and all physiologic fluids. GER was chosen as hydrolysis product to be analyzed, being detectable and quantifiable by the UV detector of the HPLC system. To this purpose, an efficacious analytical method was developed based on the use of a reverse phase C-18 HPLC column and a mobile phase constituted by a mixture of water and acetonitrile following a gradient profile allowing us to quantify both the conjugate GER-UDCA and its hydrolysis product GER in the same HPLC chromatogram in all incubation media investigated.

The solubility value of GER-UDCA in water was 439 ± 35 nM (0.23 ± 0.02 µg/mL).

The conjugate GER-UDCA was not degraded in Tris-HCl buffer (pH 7.4) during its incubation at 37°C for 8 h. This result excludes the possibility that factors other than homogenates enzymatic pools might be responsible for the GER-UDCA hydrolysis in rat brain and liver homogenates (see below), prepared as Tris-HCl suspension.

The kinetic studies in rat brain and liver homogenates were performed by adding the stock solutions (1% v/v GER or GER-UDCA $5 \cdot 10^{-2}$ M in DMSO) in the incubation media, taking into account that the protein contents in physiologic fluids allowed solubilization of the lipophilic conjugate [25]. In these incubation media GER showed high stability within 6 h, whereas the conjugate GER-UDCA appeared degraded. In particular, Fig. 2A reports the degradation profile of GER-UDCA in rat liver homogenate whose half-life is 36.5 ± 2.1 min. This degradation followed a pseudo first-order kinetic, confirmed by the linear pattern of corresponding semilogarithmic plot ($n = 8$, $r = 0.984$, $p < 0.0001$) suggesting, therefore, that conjugate degradation is governed by a hydrolysis process. The hydrolysis of GER-UDCA was confirmed by the GER appearance in incubation media with amounts increasing during time, as reported in Fig. 2B. In particular, more than the 95% of GER-UDCA appeared hydrolyzed after incubation for 180 min in rat liver homogenate. This degradation profile was not significantly changed in the presence of unloaded PLGA or SLN particles (data not shown).

Similarly, the conjugate GER-UDCA exposed to rat brain homogenate underwent hydrolysis, as reported in Fig. 3, however the reaction rate was markedly lower in comparison with the degradation in liver homogenate. Indeed, after 360 min of

incubation, about the 30% of the conjugate appeared hydrolyzed, with the release of a corresponding amount of GER.

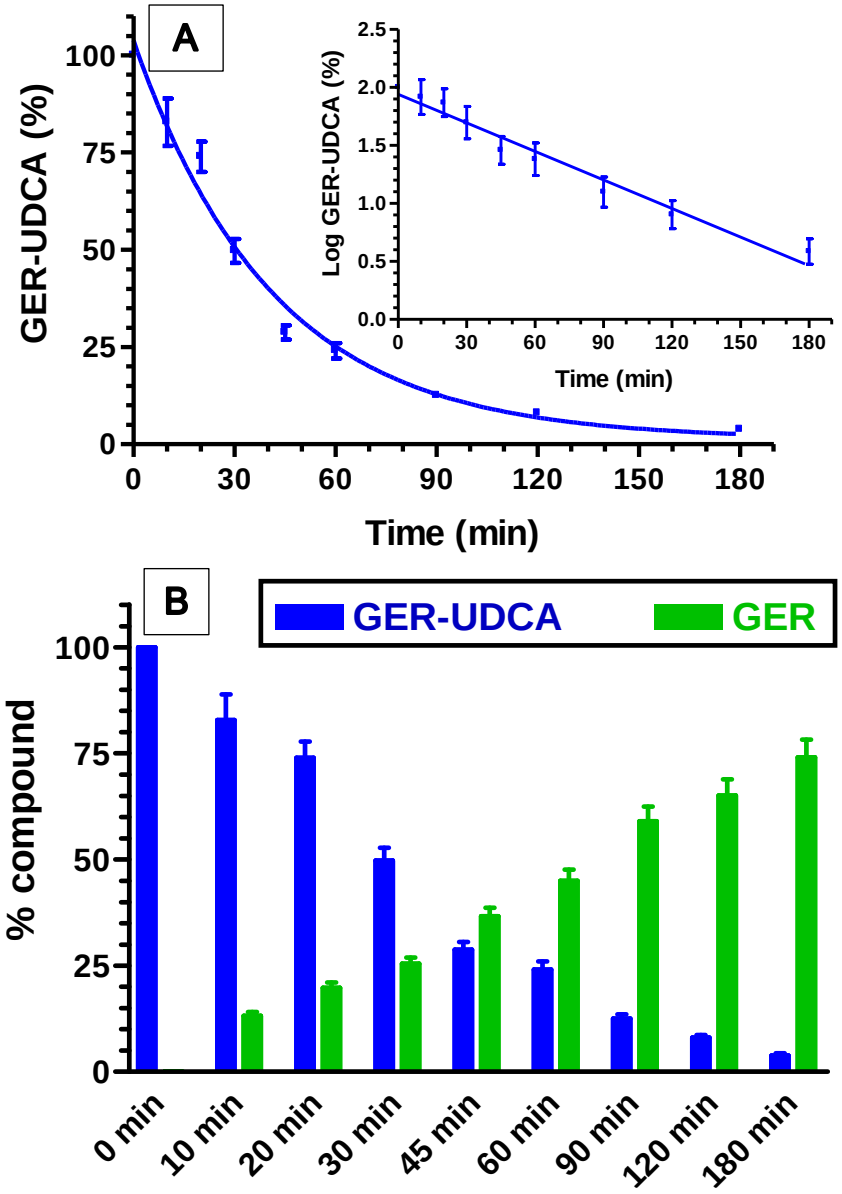

Fig. 2. [A] Hydrolysis profile of the prodrug GER-UDCA incubated in rat liver homogenate and the corresponding semilogarithmic plot (inset), whose linearity (n = 8, r = 0.984, $p < 0.0001$) indicate a pseudo first order kinetic process. **[B]** Hydrolysis profile of the prodrug GER-UDCA represented with the corresponding appearance profile of GER during incubation in rat liver homogenate. All the values are reported as the percentage of the overall molar amount of incubated prodrug and as the mean ± SD of three independent experiments.

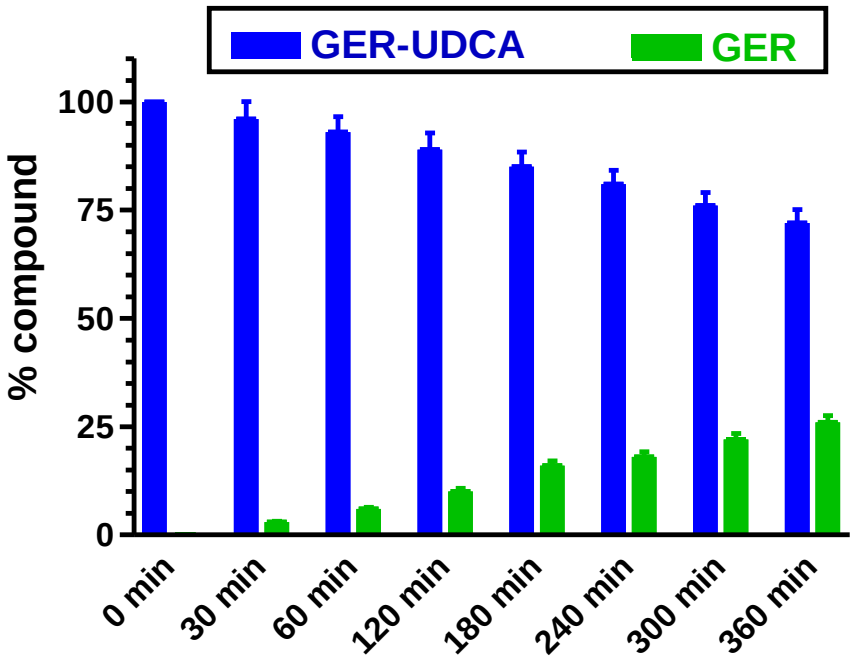

Fig. 3. Hydrolysis profile of the prodrug GER-UDCA represented with the corresponding appearance profile of GER during incubation in rat brain homogenate. All the values are reported as the percentage of the overall molar amount of incubated prodrug and as the mean ± SD of three independent experiments.

3.3 Characterization of GER and GER-UDCA-loaded nanoparticles

Particle size, PDI and drug content of both lipid (SLNs) and polymeric (NPs) nanoparticles are reported in Table 1. GER and GER-UDCA content is expressed as encapsulation efficiency (EE%) before freeze-drying and drug loading (DL%) after freeze-drying.

Both SLNs and NPs showed average particle size below 200 nm with good homogeneity, as indicated by the PDI values lower than 0.2. GER quantification before freeze-drying process showed a high EE%, over 60%. However, for both samples, the DL% after freeze-drying process was not quantifiable, being near zero. Several modifications of the formulation process were adopted but negligible amounts of drug were found after freeze drying process in all cases (see supplementary materials, Table 2S). In light of that, formulating GER-loaded SLNs and NPs was not viable.

Conversely, the EE% values of GER-UDCA-SLNs and GER-UDCA-NPs before freeze-drying were 94.5 ± 2.6% and 89.3 ± 3.2%, respectively and the DL% values of

freeze-dried samples were 6.2 ± 0.6% (GER-UDCA-SLNs) and 12.1 ± 1.4% (GER-UDCA-NPs), demonstrating that the freeze-drying process did not remove GER-UDCA from these formulations as occurred for GER with the native compound.

GER-UDCA-SLNs and GER-UDCA-NPs showed mean particle size of 121 ± 8.4 and 181 ± 5.9 nm with polydispersity index less than 0.2, and zeta potential around -22.5 ± 7.7 and -26.7 ± 6.5 mV, respectively. It was observed that the incorporation of GER-UDCA into both nanosystems increased their size compared to unloaded formulations ($p < 0.05$). On the contrary, the particle homogeneity was not significantly affected by the addition of the drug, maintaining the narrow distribution for both the delivery systems (Table 1). Additionally, morphology analysis showed spherical shape and homogeneous size of the nanoparticles (Fig. 4).

In vitro release experiments demonstrated a low dissolution rate of free GER-UDCA, where less than 10% of the prodrug was dissolved in 8 h. On the other hand, GER-UDCA release from nanoparticles showed a high and quick burst effect of approximately 29% and 68% at 15 min for GER-UDCA-NPs and GER-UDCA-SLNs, respectively (Fig. 5). In addition, the overall GER-UDCA released within 8 h from NPs was about 40%, while for SLNs a minimum increase of prodrug release was observed over time, following the burst effect. However, the cumulative release of GER-UDCA from SLNs within 8 h was about 35% higher than NPs, mainly due to initial burst effect.

Table 1.

Particle size, polydispersity index (PDI), Entrapment Efficiency (EE%) and Drug Loading (DL%) of lipid (SLNs) and polymeric (NPs) nanoparticles.

Formulation	Size (nm)	PDI	Zeta (mV)	EE%	DL% (w/w)
Unloaded SLNs	104 ± 5.3	0.148 ± 0.02	-20.0 ± 5.5	-	-
GER-SLNs	140 ± 7.5	0.110 ± 0.01	-13.5 ± 3.6	82.4 ± 0.5	NV
GER-UDCA-SLNs	121± 8.4*	0.164 ± 0.03	-22.5 ± 7.7	94.5 ± 2.6	6.2 ± 0.6
Unloaded NPs	144 ± 9.2	0.052 ± 0.01	-23.6 ± 4.6	-	-
GER-NPs	190 ± 7.0	0.117 ± 0.08	-23 ± 4.2	65.8 ± 1.5	NV
GER-UDCA-NPs	181 ± 5.9$^{\#}$	0.060 ± 0.02	-26.7 ± 6.5	89.3 ± 3.2,	12.1 ± 1.4

Data represents mean ± SD ($^{*;\#}$ $p < 0.05$); NV: negligible value

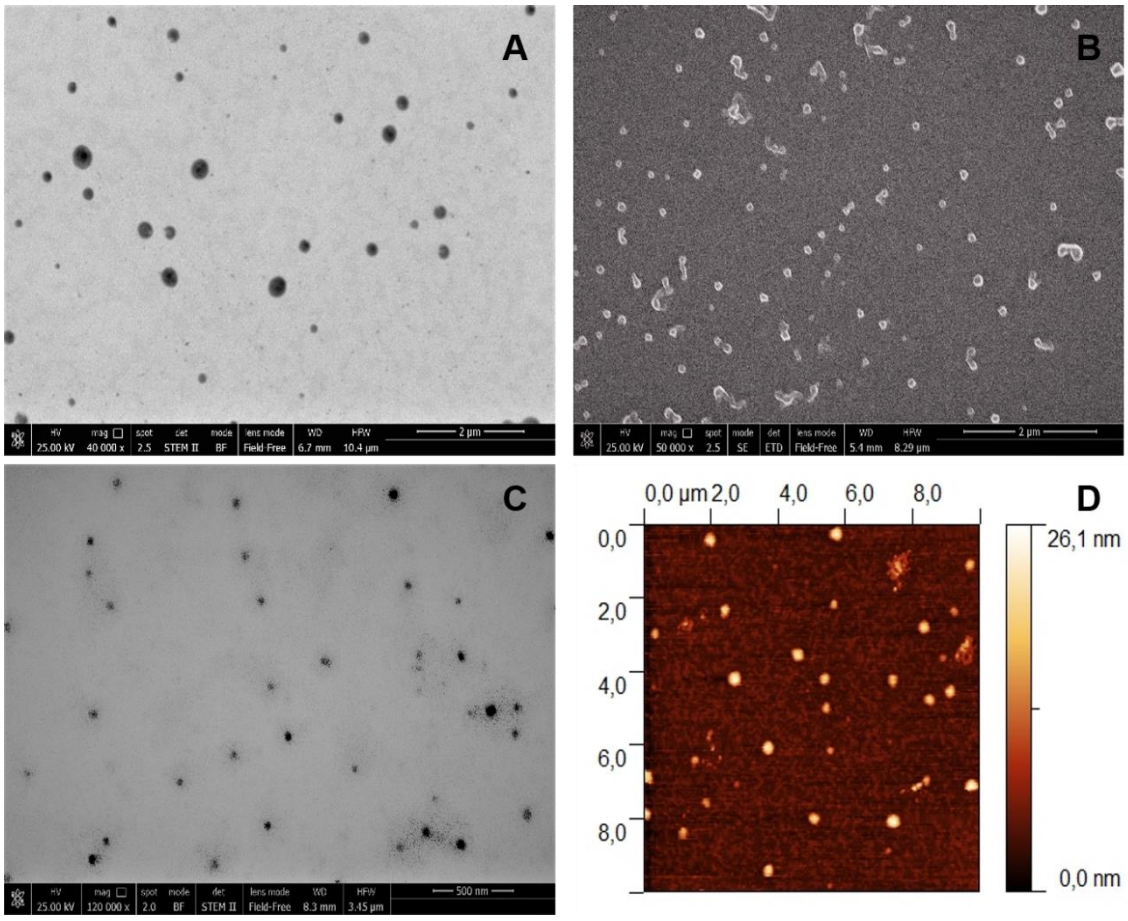

Fig. 4. Microscopy images of GER-UDCA nanoparticles showing a spherical shape and size homogeneity. A-B: Trasmission electron microscopy (TEM) and Scanning electron microscopy (SEM) images of GER-UDCA-NPs C-D: TEM and atomic force microscopy (AFM) imag

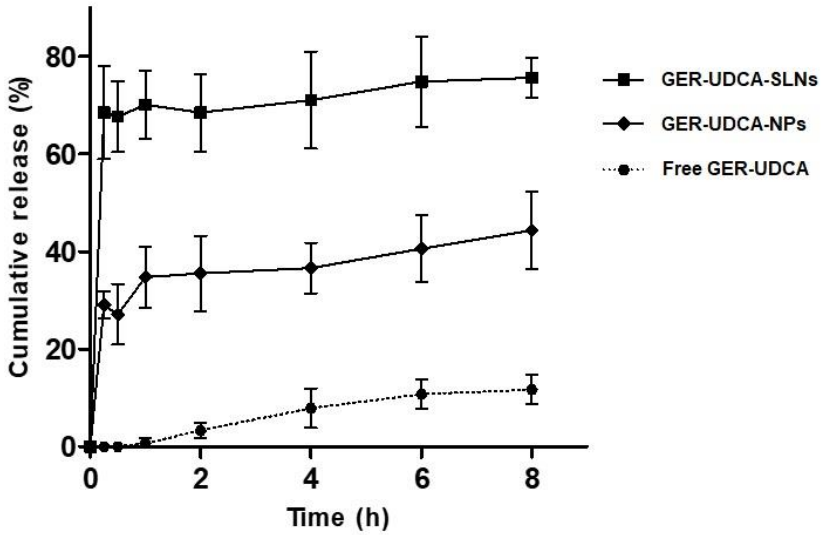

Fig. 5. *In vitro* cumulative GER-UDCA release from formulations in aqueous medium with 5 mM SDS at 37°C (n=3). Data represent mean ± SD.

3.4. Hydrolysis studies of free and encapsulated GER-UDCA in rat liver homogenates.

In order to evaluate the ability of PLGA and lipid nanoparticles to protect and stabilize the prodrug in physiologic environments, we decided to compare the hydrolysis rate of free and encapsulated GER-UDCA in the tissue homogenates above described. In particular, rat liver homogenates were selected for the study, because in the hydrolysis rate of the prodrug is faster in this biological preparation than in brain homogenates. ~~In particular~~, As reported in Fig. 6, after 120 min of incubation about 90% of the solubilized free prodrug was hydrolyzed with the apparence of corresponding amounts of the hydrolysis product GER. Similar results were observed after 120 min of incubation of the GER-UDCA-SLNs. On the contrary, following 120 min incubation of GER-UDCA-NPs in rat liver homogenates, about 85% of the prodrug was still present, with corresponding poor amounts of GER produced by hydrolysis (about 15%; Fig. 6).

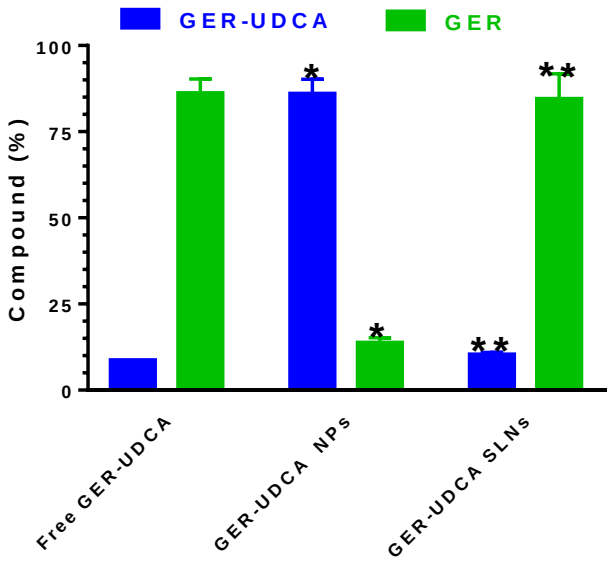

Fig. 6. Hydrolysis in rat liver homogenates, after incubation for 120 min of free or encapsulated GER-UDCA in PLGA or SLNs particles. All GER-UDCA and GER values are reported as the percentage of the overall amount of incubated prodrug and as the mean ± SD of three independent experiments.

*P< 0.001 versus Free GER-UDCA; **P> 0.05 versus Free GER-UDCA.

These results suggest that the ability of NPs and SLNs to stabilize the prodrug in rat liver homogenates is strongly related to their capacity to control the relase of the encapsulated GER-UDCA, as reported in Fig. 5. In particular, the ability of SLNs to increase the dissolution rate of GER-UDCA is further confirmed.

Overall, these data suggest that the rat liver homogenate can represent an optimal model to evaluate nanoparticle properties in physiologic environments. In particular, when the nanoparticles are able to control the prodrug relase (*e.g.* PLGA), they induce its protection from degradation, thus inducing a low hydrolysis rate. On the other hand, when the nanoparticles are able to induce a fast dissolution of the prodrug (*e.g.* SLNs), its hydrolysis is rapid. This last type of formulation may be particularly indicated for nasal administration, allowing a fast dissolution of the prodrug in nasal cavity, with consequent efficacious targeting in the CNS.

3.5. In vivo GER and GER-UDCA ~~nasal~~ administration.

3.5.1. Intravenous administration of GER-UDCA

GER-UDCA was firstly administered to rats by intravenous infusion at the dose of 500 μg (*i.e.* the same used for nasal administration of the GER-UDCA-loaded SLNs, see below). The higher GER-UDCA concentration detected in whole blood was 13.1 ± 0.8 μg/mL. This value decreased during time and blood GER-UDCA concentartion was not quantifiable at the 60 min time-point. GER was not detected in whole blood during this range of time, while both GER and GER-UDCA were not detected in CSF within 90 min after the end of infusion.

In order to better evaluate the pharmacokinetics of GER-UDCA after intravenous infusion to rats, a 2.5 mg dose was also administered. Under these experimental conditions, the rat blood GER-UDCA concentration at the end of infusion was 73.5 ± 5.6 μg/mL and it decreased during time (Fig. 7A) with an apparent first order kinetic confirmed by the linearity of the semilogarithmic plot reported in the inset of Fig. 7A (n = 8, r =0.993, P < 0.0001), and a half-life ($t_{1/2}$) of 21.6 ± 0.8 min. The

pharmacokinetic data (Table 2) indicate a clearance (CL) value of 4.35 ± 0.15 mL·min^{-1}·Kg^{-1} and a volume of distribution (Vd) value of 136 ± 9 mL·kg^{-1}.

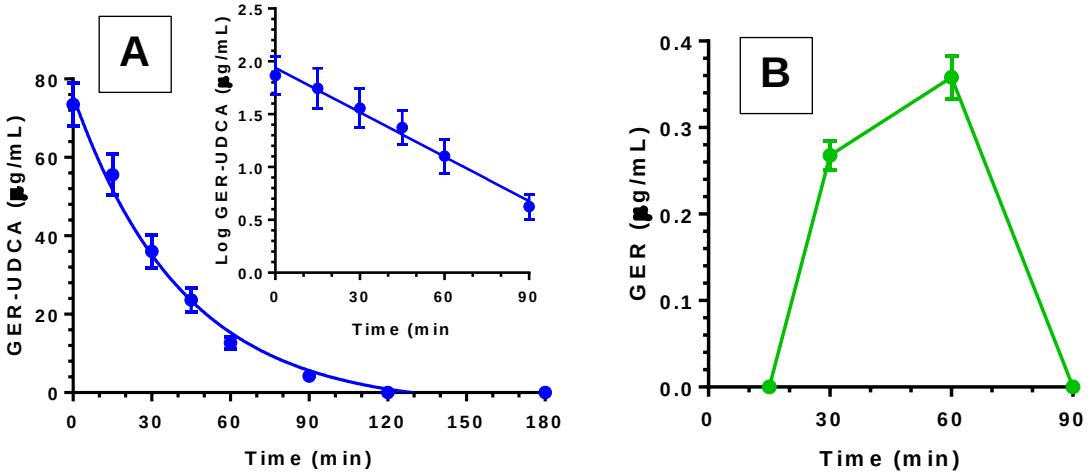

Fig. 7. [A] Plasma elimination profile of GER-UDCA intravenously infused to rats at 2.5 mg dose. The elimination followed an apparent first order kinetic, confirmed by the semilogarithmic plot reported in the inset (n = 8, r = 0.993, P < 0.0001). The calculated half-life of GER-UDCA was 21.6 ± 0.8 min. **[B]** Rat blood GER amounts following the intravenous infusion of GER-UDCA (2.5 mg). All data are expressed as the mean ± SD of four independent experiments.

Finally, the intravenous infusion of 2.5 mg of GER-UDCA allowed to detect GER in rat blood at 30 and 60 min, with values around its LOQ (about 0.3 µg/mL, Fig. 7B).

Table 2.

Pharmacokinetic parameters of GER-UDCA after intravenous administration of a 2.5 mg dose to rats. Data are reported as mean ± SD (n = 4). C_0: concentration at the end of infusion; AUC: area under concentration; k_{el}: elimination rate constant; $t_{1/2}$: half-life; CL: clearance; Vd: volume of distribution.

C_0 (µg/mL)	AUC (µg·mL^{-1}·min)	k_{el} (1/min)	$t_{1/2}$ (min)	CL (mL· min^{-1}· kg^{-1})	Vd (ml/kg)
73.5 ± 5.6	2875 ± 95	0.032 ± 0.0018	21.6 ± 0.8	4.35 ± 0.15	136 ± 9

3.5.2. Nasal administration of GER and GER-UDCA

GER was nasally administered at the dose of 4 mg/kg as emulsified formulation in a mixture of glycerol and water. Fig. 8 reports the GER concentrations detected during time in CSF of rats, following the nasal administration. The GER values detected were 4.3 ± 0.70 and 2.16 ± 0.32µg/mL at 30 and 60 min, respectively, as evidenced in the inset of Fig. 8. However, a drastic increase of GER concentration was evidenced in CSF at 90 min, (122 ± 15 µg/mL) whose value appeared up to 56 times higher than those detected at 30 or 60 min. These data suggest that the GER ability to permeate across olfactory mucosa drastically increased 1 h after its intranasal administration.

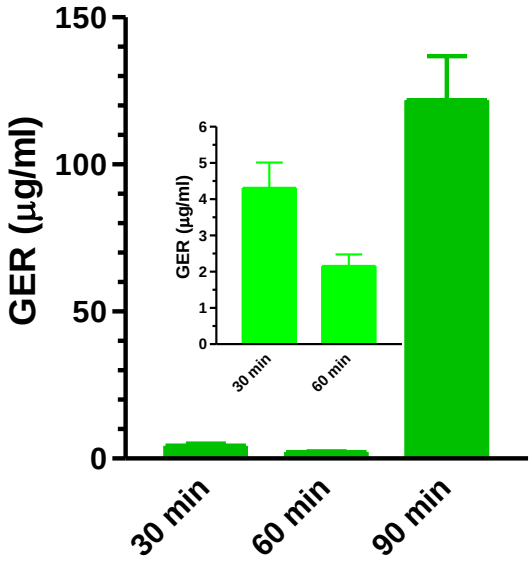

Fig. 8. GER concentrations (µg/mL) detected in the CSF of rats after nasal administration of a 1 mg dose as emulsified formulation in a mixture of glycerol and water. Data are expressed as the mean ± SD of at least four independent experiments.

GER-UDCA-SLNs demonstrated not only a high EE% but also the ability to induce a fast release of GER-UDCA. Therefore, GER-UDCA was nasally administered at the dose of 2 mg/kg as a water suspension of GER-UDCA-SLNs in order to verify its potential uptake in the CNS.

The GER-UDCA-SLNs nasal administration produced detectable amounts of GER-UDCA in the CSF of the rats, as reported in Fig. 9. In particular, GER-UDCA concentrations in the CSF were 4.65 ± 0.52 µg/mL at 30 min then the concentration values slowly decresed to 1.1 ± 0.10 µg/mL at 150 min after nasal administration. After

180 min GER-UDCA concentration was not detectable. No GER amounts were detected in CSF of rats wihin 180 min after nasal administration of SLNs. Moreover, no GER or GER-UDCA amounts were detected in the bloodstream within 180 min after nasal administration of the particles. The AUC value in CSF obtained by nasal administration of GER-UDCA-SLNs (500 µg of GER-UDCA for rat) was 389 ± 15 $\mu g \cdot mL^{-1}$ min (736 ± 28 µM min).

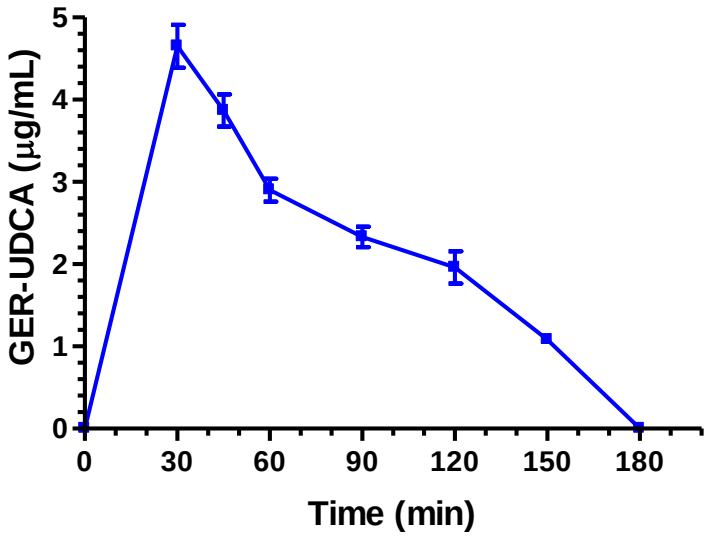

Fig. 9. GER-UDCA concentrations (µg/mL) detected in the CSF of rats after nasal administration of a 500 µg dose as GER-UDCA-SLNs . Data are expressed as the mean ± SD of at least four independent experiments.

3.6. Histopathological examinations of nasal mucosae

The histopathological evaluation of rat nasal mucosae was performed after 2 h from the intranasal administration of free GER, GER-UDCA-SLNs, PBS 7.4 and isopropyl alcohol (Fig. 10). No signs of damage were detected on the nasal mucosa after the administration of both PBS 7.4 (negative control, Fig. 10A) and GER-UDCA-SLNs (Fig. 10C), since a well-preserved epithelial lining of the olfactory region was evident. On the contrary, after the administration of both the positive control (isopropyl alcohol,

Fig. 10B) and free GER (Fig. 10D), a separation of pseudostratified columnar epithelium from basement membrane was observed.

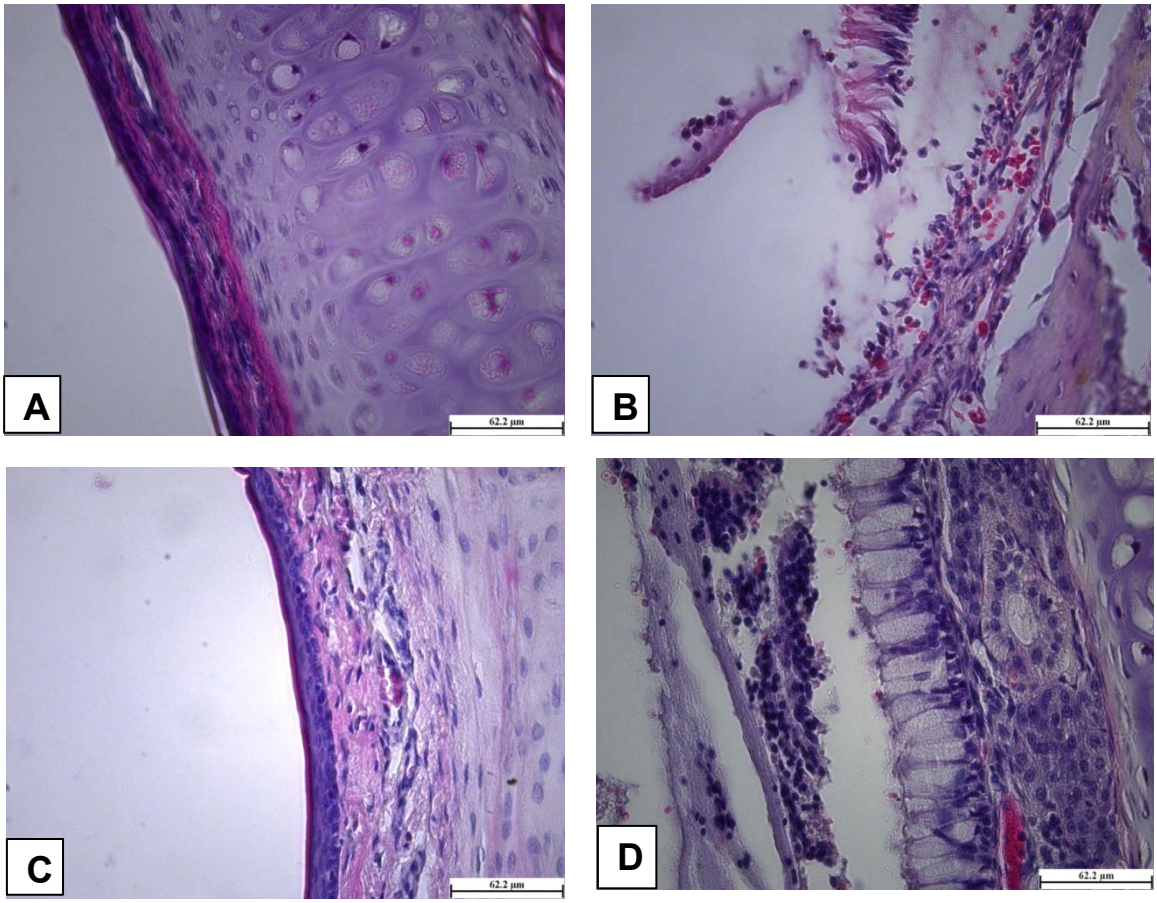

Fig. 10. Representative histological sections of nasal mucosae of rats 2 h after intranasal administration of [A] PBS 7.4 (as negative control), [B] isopropyl alcohol (as positive control), [C] GER-UDCA-SLNs and [D] free GER. Magnification: 40X. Scale bars = 62.2 µm.

4. Discussion

Therapeutic strategies able to counteract neuroinflammation or to induce mitochondrial protective effects appear promising to prevent and/or to reduce PD progression. Among other agents, natural compounds possessing these properties such as GER, an abundant component of essential oils [11], and UDCA, a bile acid, have been recently proposed. In fact, in a mice model of PD, GER alleviated the

neuromuscular impairment [10] induced by the administration of 1-methyl-4-phenyl-1,2,3,6-tetrahydropyridine (MPTP), while UDCA has been proposed as an encouraging neuroprotective drug, being able to induce beneficial effects on dopaminergic neuron mitochondrial functions [13,26].

Both GER and UDCA penetrate the CNS from the bloodstream and their ability to reach the cerebrospinal fluid has been demonstrated [12, 16,27]. Their neuroprotective effects could be, therefore, exerted following the drug oral administration, although very high doses (up to 200 mg/kg or 50 mg/kg per day for GER or UDCA, respectively) would be required [8, 16]. Moreover, GER appears quickly eliminated from the body after its oral administration, showing a very short half-life (about 12 min) at systemic and central levels in rats [12]. These aspects could compromise the use of these natural potential drugs for long-term therapies against PD, thus prompting the development of new strategies to improve their brain delivery and survival after administration. In this context, nose-to-brain delivery represents an interesting approach since it permits a direct transport of neuroactive agents to CNS, thus allowing to achieve therapeutic compound CNS concentrations after the administration of relatively low dosages [28]. In particular, the olfactory and trigeminal pathways allow to deliver drugs or prodrugs from nose to CNS within few minutes. These pathways encompass drug transport across the olfactory mucosa, or extracellular routes, such as the transport via olfactory neurons, or trigeminal nerves [29,30], avoiding the axonal transport which, instead, requires endocytosis processes and some days to be completed [31]. Unfortunately, the nasal administration of GER could be associated with several issues. Firstly, GER is liquid at room temperature and causes high mucosal irritability [32]. Moreover, its poor water solubility (100 mg/L) and high partition coefficient (2.65) [33] generally induce its separation from aqueous formulations with consequent administration difficulties and mucosal damages [32]. This latter aspect also emerged in the present study, following the rat nasal administration of GER (4 mg/kg) as a water emulsion in the presence of glycerol. This formulation was previously used for oral GER (50 mg/kg) administration and allowed to detect the compound in rat CSF at concentrations ranging from about 0.8 to 2.5 µg/mL within 45 min after the administration [12]. ~~Under this experimental condition~~ Following the GER nasal administration, in fact, the CSF GER concentrations ranged between ~2 and ~4 µg/mL within 60 min ~~after the nasal administration~~, but at 90 min they suddenly increased to ~120 µg/mL, suggesting a drastic change of permeability of

nasal mucosa. In line with this scenario, the histopathological analysis of nasal mucosa of rats evidenced serious mucosal damages 120 min after the administration of this GER emulsion (Fig. 10D) although the intranasal GER dose was about ten times lower than the oral one. Another issue possibly related to GER nasal administration is its relative high volatility that seems to preclude the compound encapsulation in polymeric or lipid nanoparticulate systems. In the present study, this aspect emerged by the results obtained after the design and development of biocompatible delivery nanocarriers for the nose-to-brain delivery of GER. Specifically, lipid-based (SLNs), obtained with compritol, and polymeric (NPs) nanoparticles, based on PLGA, were prepared by melt-emulsification with solvent evaporation and nanoprecipitation techniques, respectively, to obtain particles in the nanometric range. Compritol is composed by glycerol mono, di- and tri-behenate and it was selected for its high biocompatibility [34] as well as PLGA polymer, approved by FDA for formulation development [35]. In GER-loaded nanoparticles, the compound content was relatively high before freeze-drying, but following this process it appeared negligible, regardless the kind of matrix material (see supplementary materials). The use of mannitol and trehalose as cryoprotectant was also tested, in order to prevent potential particle aggregation and fusion and to protect the nanoparticles from the mechanical stress of ice crystals [36]. Unfortunately, this strategy did not avoid GER loss, suggesting that this phenomenon is due to GER volatility (*data not shown*). In the attempt to overcome these limitations, we have previously proposed a formulation based on chitosan oleate as surfactant, which allows to obtain a GER emulsion in water characterized by droplets lower than 1 µm with high stability during time. The nasal administration of this formulation (1 mg/kg of GER) to rats induced quite high GER concentrations in CSF (> 100 µg/mL); unfortunately, the effects of this formulation on nasal mucosa have not been yet elucidated and, therefore, cannot be excluded. [27]. Based on these issues, in the present study we explored the possibility of intranasal administration of an innovative GER-UDCA prodrug as useful strategy to improve the CNS targeting of GER and UDCA co-administration. The prodrug approach appeared suitable to this aim, being often used to avoid clinical limitations related to the therapies based on some neuroactive drugs [37,38]. As an example, this strategy can allow to circumvent the active efflux transporters expressed on the barriers between the bloodstream and the CNS [25], as well as to prolong the activity of drugs with short half-lives [39]. Besides these advantages, we have recently demonstrated that some prodrugs are particularly suitable to be included in micro or

nano-particulate formulations in order to enhance the brain targeting of neuroactive agents following nasal administration [21,40,41].

We have firstly provided GER and UDCA ester conjugation in order to obtain the GER-UDCA prodrug, potentially releasing both compounds after its hydrolysis by endogenous esterases [42]. The GER-UDCA conjugate showed high stability in Tris-HCl buffer. A similar result was previously obtained with GER incubated in phosphate buffer saline (PBS, pH 7.4) [12]. On the other hand, in rat liver or brain homogenates the conjugate was hydrolyzed, evidencing its aptitude to release GER and UDCA in physiologic environments. GER-UDCA prodrug appears, therefore, potentially able to release both GER and UDCA in the liver or brain, in dependence of its ability to target these compartments. The lower hydrolysis rate of the prodrug detected in brain homogenates with respect to liver homogenates suggests that GER-UDCA may induce a controlled release of GER and UDCA in the CNS, allowing their prolonged activity during time. Based on these properties, GER-UDCA appeared a prodrug suitable to be included in nanoparticulate systems, in order to obtain nasal formulations for its targeting in the CNS. Interestingly, the usefulness of nanoparticulate nasal formulations has been evidenced for the nose to brain delivery of dopamine, against the PD symptoms [43]. Differently from GER, GER-UDCA prodrug is not volatile and appears semisolid with very low water solubility. These last properties make difficult its intranasal administration in the free form. Consequently, biocompatible delivery nanocarriers for the nose-to-brain delivery of GER-UDCA were designed and developed with the same procedures and materials used for GER encapsulation (see above). GER-UDCA-SLNs, based on compritol, and GER-UDCA-NPs, based on PLGA, were characterized demonstrating that they have an average diameter below 200 nm. The negative zeta potential of formulations may be attributed to lipid and polymer nature, which guarantees their physical stability, since the charge repulsion between the nanoparticles avoids their aggregation. For a nose to brain delivery of nanoparticles, both size and zeta potential influence and determine the brain distribution of drugs. Particles around 100 nm have been demonstrated to increase brain drug concentration compared to other administration routes [44,45]. Regarding the superficial charge, the issue is controversial. The drug absorption is influenced by a large number of different parameters that makes difficult to compare different results. Overall, both negative and positive charged nanoparticles have been established to increase brain drug concentration compared to other routes or to drug solutions [44-46].

High EE% of the lipophilic GER-UDCA in both nanocarriers used in this study were obtained, consistent with the expectations. In fact, during nanoprecipitation lipophilic drugs do not migrate to aqueous phase but interact with the polymeric matrix where they are encapsulated [47]. In the case of SLNs, the evaporation of organic solvent spontaneously occurs in precipitation of lipids along with the drug, since lipophilic compounds generally show higher affinity for the lipid dissolved into organic phase, than for water [48]. Nevertheless, DL% values showed that the use of GER-UDCA was efficient to improve the amount of GER in the freeze-dried nanoparticles, confirming the reduction of GER volatility when conjugated with UDCA.

In vitro release data showed a higher dissolution rate of GER-UDCA from the present formulations compared to the free prodrug in its semisolid form. In fact, nanoparticles have been applied for enhancing solubility of poorly water-soluble drugs, since the reduction of particle size increases their surface area, which would be related to the higher drug dissolution rate [49,50]. In particular, our results clearly evidenced this solubility effect for GER-UDCA-SLNs. The high and quick burst effect obtained with this formulation suggests that important amounts of GER-UDCA are placed on the surface of SLNs or just nearby, rather than entrapped in their lipid matrix. On the other hand, the ability of NPs to better control the prodrug release, suggests higher core distribution of GER-UDCA than in SLNs. Remarkably, the high concentration of surfactants used for SLNs manufacturing may contribute to accelerate drug release from the nanoformulations [51]. Rapid or prolonged therapeutic effects may be therefore obtained by the different release patterns of SLNs and NPs that allow to deliver the prodrug at different rates.

The stability studies of free and encapsulated GER-UDCA in rat liver homogenates evidenced the ability of NPs to strongly reduce the hydrolysis of GER-UDCA in a physiological environment, whereas this effect appeared very poor with SLNs, confirming their ability to promote a prompt dissolution of the prodrug. This prompt dissolution can be very useful in order to induce a nose-to-brain delivery of GER-UDCA, based on diffusional mechanisms across nasal mucosae. The SLNs were therefore selected as the formulation suitable for nasal administration of the prodrug and their potential ability to promote its uptake in CNS was evaluated.

Following the administration in the rat nostrils of GER-UDCA-SLNs suspension, containing a prodrug dose of 500 μg (*i.e.* a dose similar to those we previously used for micro- and nanoformulation of prodrugs [21,28,41]), GER and

prodrug concentrations in CSF and bloodstream were measured. It was not possible to perform a comparison with raw GER-UDCA, being its semisolid and highly adhesive form not suitable for nasal administration.

The compritol based SLNs induced the uptake of the prodrug in the CSF, allowing to obtain concentrations up to ~5 µg/mL within 30 min after nasal administration. These data confirm the ability of GER-UDCA-SLNs to induce the delivery in nasal mucosa of prodrug amounts ready to be targeted in the CSF, probably by promoting its dissolution rate. Interestingly, no GER or GER-UDCA amounts were detected in the bloodstream of rats, following the nasal administration of the nanoparticulate suspension. Similarly, these compounds were not detected in CSF following the intravenous administration of the same dose of GER-UDCA (500 µg). As this could be possibly due to the potential quick hydrolysis and high volume of distribution of GER-UDCA, we also evaluated the pharmacokinetic parameters of GER-UDCA following the intravenous administration of a higher prodrug dose (2.5 mg dose). Data reported in Table 1 indicate that the prodrug half-life is about 20 min, while the volume of distribution and clearance values are about 150 mL/kg and 5 mL$\cdot$ min$^{-1}\cdot$ kg^{-1}, respectively. Literature data report rat volume of distribution values of drugs ranging from 100 mL/kg to 100 L/kg orders of magnitude. Similarly, clearance values are reported ranging from 1 mL$\cdot$ min$^{-1}\cdot$ kg^{-1} to 10 L$\cdot$ min$^{-1}\cdot$ kg^{-1} orders of magnitude [52-53]. The pharmacokinetic data reported in Table 2 indicate, therefore, that the elimination rate of GER-UDCA from the rat bloodstream is relatively slow. This profile appears, indeed, markedly different from that of a similar prodrug (UDCA-AZT), obtained by the conjugation of zidovudine (AZT) with UDCA, whose hydrolysis in rat whole blood showed a half-life of few seconds [25]. Moreover, the data reported in Table 2 also suggest that GER-UDCA poorly migrates to peripheral tissues, showing a relatively small volume of distribution. This pharmacokinetic profile can be related to a poor permeation coefficient of the prodrug, possibly due to its relatively high molecular weight (528 Da). In this context, we have previously demonstrated that AZT showed a strong decrease of its permeation coefficient across cell monolayers when conjugated to UDCA [25].

Finally, the intravenous infusion of the 2.5 mg dose of GER-UDCA allowed to detect GER in rat blood at 30 and 60 min, with values around its LOQ (about 0.3 µg/mL, Fig. 7B). The poor amounts of GER detected in the blood of rats are probably

due to its higher elimination rate ($t_{1/2}$ = 12,5 ± 1.5 min) [12] with respect to the elimination rate of GER-UDCA, whose half-life is 21.6 ± 0.8 min.

Overall, these data ~~emphasizes the ability of~~ suggest that SLNs promote a selective uptake of GER-UDCA in CSF, thus indicating the existence of a direct nose-CNS pathway for this prodrug. This view is also supported by the lack of detectable GER-UDCA concentrations in rat blood after the prodrug nasal administration. In fact, it seems likely that this could not be related to the high volume of distribution and/or rapid clearance of GER-UDCA, but rather to its incapability to pass from brain into peripheral circulation.

Moreover, following the nasal administration of SLNs, GER-UDCA permanence in CSF appeared sensibly prolonged (about 2 h) in comparison to the CSF permanence of GER administered by oral route [12].

It may be intersting to observe that GER-UDCA AUC value in CSF of rats (736 ± 28 µM·min) obtained after nasal administration of SLNs is significantly higher ($P < 0.001$) than that obtained by the oral administration of 12,5 mg of GER (473 ± 23 µM·min) [12], a dose about 100 times higher, in molar terms, than that of the prodrug nasally administered (please see Supplementary Methods for further details).

The absence of GER in CSF, following the nasal administration of GER-UDCA, suggests that the prodrug hydrolysis can be localized in the brain parenchima, as evidenced by the prodrug hydrolysis detected in rat brain homogenates. In view of this evidence, further experiments in animal PD models are necessary to evaluate the efficacy of this new therapeutic approach.

Finally, the histopathological examinations of nasal mucosa highlighted the safety of the intranasal administration of GER-UDCA-SLNs in comparison to free GER and isopropyl alcohol (positive control). Indeed, neither mucosa damage nor alteration in the epithelial lining was observed, as the integrity of both the pseudostratified columnar epithelium and the basement membrane was maintained (Fig. 10C). These results indicate the high biocompatibility of GER-UDCA-SLNs with respect the GER nasal formulation. For the sake of clarity, it is relevant to remark that pharmacokinetic results and histopathological data were obtained in two different rat strains (i.e. Sprague-Dawley and Wistar rat, respectively). Although these rat strains are the most widely used ones, usually not discriminated in research, and there are no histopathological differences between them it will be important, in a further study, to confirm the present histopathological results in Sprague-Dawley rats.

5. Conclusions

To achieve brain targeting via intranasal administration, we propose lipid nanoparticles containing a new prodrug obtained by the conjugation of GER with UDCA, two natural compounds known to prevent and counteract PD. Even if *in vitro* experiments demonstrate the ability of the prodrug to be hydrolyzed in physiologic environments, its sticky consistence and very poor solubility hindered its intranasal administration. The encapsulation of GER-UDCA in polymeric or lipid nanoparticles induced a significant increase of its dissolution rate in aqueous solvent. In particular, nasal administration of GER-UDCA-SLNs demonstrated the ability of SLNs to induce prodrug permeation from nose to CSF of rats, without inducing mucosal irritation. In conclusion, these data suggest the potential ability of this formulation to induce drug central effects, in the absence of peripheral undesired phenomena indicating that the prodrug nanoencapsulation could provide an effective noninvasive approach to encourage the access of GER and UDCA to the brain for treatment of PD. Future experiments in animal PD models are needed to demonstrate the efficacy of this therapeutic approach.

Acknowledgments

Support from the University of Ferrara, Italy (2018-FAR.L-DA_002) in the frame of the project FAR2018 is gratefully acknowledged. This work was also financially supported by the University of Modena and Reggio Emilia, (FAR2019-DSV-Leo). Moreover, funding from CAPES (Coordenação para o Aperfeiçoamento de Pessoal de Nível Superior) - (financing code 001) and FAPEG (Fundação de Amparo à Pesquisa do Estado de Goiás) supported the work. The authors thank Daniel Graziani for the histology processing and image acquisition.

References.

[1] J. Parkinson, An essay on the shaking palsy. 1817, J. Neuropsychiatry Clin. Neurosci. 14 (2) (2002) 223–236. doi: 10.1176/jnp.14.2.223

[2] G. Gelders, V. Baekelandt, A. Van der Perren, 2018. Linking neuroinflammation and neurodegeneration in Parkinson's disease, J. Immunol. Res. 4784268. doi: 10.1155/2018/4784268

[3] D. Kempuraj, R. Thangavel, P. A. Natteru, G.P. Selvakumar, D. Saeed, H. Zahoor, S. Zaheer, S.S. Iyer, A. Zaheer, Neuroinflammation induces neurodegeneration, J. Neurol. Neurosurg. Spine 1 (1) (2016) 1–15.

[4] H. Büeler, Impaired mitochondrial dynamics and function in the pathogenesis of Parkinson's disease, Exp. Neurol. 218 (2) (2009), 235–246. doi: 10.1016/j.expneurol.2009.03.006.

[5] L. Zuo, M.S. Motherwell, The impact of reactive oxygen species and genetic mitochondrial mutations in Parkinson's disease, Gene 532 (1), (2013) 18–23. doi: 10.1016/j.gene.2013.07.085.

[6] H.E. Moon, S.H. Paek, Mitochondrial dysfunction in Parkinson's disease, Exp. Neurobiol. 24 (2) (2015), 103–16. doi: 10.5607/en.2015.24.2.103.

[7] K.R. Rekha, G.P. Selvakumar, Gene expression regulation of Bcl2, Bax and cytochrome-C by geraniol on chronic MPTP / probenecid induced C57BL / 6 mice model of Parkinson's disease, Chem. Biol. Interact. 217 (2014) 57–66. doi: 10.1016/j.cbi.2014.04.010

[8] K.R. Rekha, G.P. Selvakumar, Geraniol ameliorates the motor behavior and neurotrophic factors inadequacy in MPTP-induced mice model of Parkinson' s disease, J. Mol. Neurosci. 51 (3) (2013) 851-862 doi: 10.1007/s12031-013-0074-9.

[9] Y.H. Siddique, F. Naz, S. Jyoti, F. Ali, A. Fatima, Rahul, S. Khanam, Protective effect of Geraniol on the transgenic Drosophila model of Parkinson's disease, Environ. Toxicol. Pharmacol. 43 (2016) 225-231. doi: 10.1016/j.etap.2016.03.018.

[10] K.R. Rekha, G.P. Selvakumar, K. Santha, R. Inmozhi Sivakamasundari, Geraniol attenuates α-synuclein expression and neuromuscular impairment through increase dopamine content in MPTP intoxicated mice by dose dependent manner, Biochem. Biophys. Res. Commun.. 440 (4) (2013) 664-670. doi: 10.1016/j.bbrc.2013.09.122.

[11] A. Lapczynski, S.P. Bhatia, R.J. Foxenberg, C.S. Letizia, A.M. Api, Fragrance material review on geraniol, Food Chem. Toxicol. 46 (11) (2008) S160–S170. doi: 10.1016/j.fct.2008.06.048.

[12] B. Pavan, A. Dalpiaz, L. Marani, S. Beggiato, L. Ferraro, D. Canistro, M. Paolini, F. Vivarelli, M.C. Valerii, A. Comparone, L. De Fazio, E. Spisni, 2018. Geraniol pharmacokinetics, bioavailability and its multiple effects on the liver antioxidant and xenobiotic-metabolizing enzymes, Front. Pharmacol. 9, 18. doi: 10.3389/fphar.2018.00018.

[13] H. Mortiboys, R. Furmston, G. Bronstad, J. Aasly, C. Elliott, O. Bandmann, UDCA exerts beneficial effect on mitochondrial dysfunction in LRRK2(G2019S) carriers and in vivo, Neurology 85(10) (2015) 846-852. doi: 10.1212/WNL.0000000000001905.

[14] H. Mortiboys, J. Aasly, O. Bandmann, Ursocholanic acid rescues mitochondrial function in common forms of familial Parkinson's disease, Brain 136 (10) (2013) 3038–3050. doi: 10.1093/brain/awt224.

[15] H.S. Chun, W.C. Low, Ursodeoxycholic acid suppresses mitochondria-dependent programmed cell death induced by sodium nitroprusside in SH-SY5Y cells, Toxicology 292 (2-3) (2012) 105–112. doi: 10.1016/j.tox.2011.11.020.

[16] G.J. Parry, C.M. Rodrigues, M.M. Aranha, S.J. Hilbert, C. Davey, P. Kelkar, W.C. Low, C.J. Steer, Safety, tolerability, and cerebrospinal fluid penetration of ursodeoxycholic Acid in patients with amyotrophic lateral sclerosis, Clin. Neuropharmacol. 33 (1) (2010) 17-21. doi: 10.1097/WNF.0b013e3181c47569.

[17] A. Roda, P. Hrelia, M. Paolini, M. Calzolari, B. Grigolo, P. Simoni, R. Aldini, G.C. Forti, Pharmacokinetics of ursodeoxycholic acid in rat, Pharmacol. Res. 23 (1991) (4) 327–335. doi:10.1016/1043-6618(91)90048-3.

[18] A.F. Hofmann, Pharmacology of ursodeoxycholicaAcid, an enterohepatic drug, Scand. J. Gastroenterol. 29 (1994 1–15. doi: 10.3109/00365529409103618.

[19] L. Illum, Is nose-to-brain transport of drugs in man a reality? J. Pharm. Pharmacol. 56 (1) (2004) 3–17. doi: 10.1211/0022357022539.

[20] N.J. Johnson, L.R. Hanson, W.H. Frey, Trigeminal pathways deliver a low molecular weight drug from the nose to the brain and orofacial structures, Mol. Pharm. 7 (3) (2010) 884–893. doi: 10.1021/mp100029t.

[21] A. Dalpiaz, L. Ferraro, D. Perrone, E. Leo, V. Iannuccelli, B. Pavan, G. Paganetto, S. Beggiato, S. Scalia, Brain uptake of a zidovudine prodrug after nasal administration of solid lipid microparticles, Mol. Pharm 11 (5) (2014) 1550–1561. doi: 10.1021/mp400735c.

~~[22] O.H. Lowry, N.J. Rosebrough, A. L. Farr, R.J. Randall, Protein measurement with the Folin phenol reagent, J. Biol. Chem. 193 (1) (1951) 265–275.~~

[22] M.P. van den Berg, S.G. Romeijn, J.C. Verhoef, F.W.H.M. Merkus, Serial cerebrospinal fluid sampling in a rat model to study drug uptake from the nasal cavity. J. Neurosci. Methods 116 (2002) (1) 99–107. doi: 10.1016/s0165-0270(02)00033-x.

[23] K. Felgenhauer, Protein size and cerebrospinal fluid composition, Klin. Wochenschr. 52 (24) (1974) 1158–64. doi: 10.1007/bf01466734.

[24] A. Madu, C. Cioffe, U. Mian, M. Burroughs, E. Tuomanen, M. Mayers, E. Schwartz, M. Miller, Pharmacokinetics of fluconazole in cerebrospinal fluid and serum of rabbits: validation of an animal model used to measure drug concentrations in cerebrospinal fluid, Antimicrob. Agents Chemother. 38 (9) (1994) 2111–2115. doi: 10.1128/aac.38.9.2111.

[25] A. Dalpiaz, G. Paganetto, B. Pavan, M. Fogagnolo, A. Medici, S. Beggiato, D. Perrone, Zidovudine and ursodeoxycholic acid conjugation: design of a new prodrug potentially able to bypass the active efflux transport systems of the central nervous system, Mol. Pharm. 9 (4) (2012) 957–968. doi: 10.1021/mp200565g.

~~[27] H. Yokoyama, H. Kuroiwa, R. Yano, Targeting reactive oxygen species, reactive nitrogen species and inflammation in MPTP neurotoxicity and Parkinson's disease, Neurol. Sci. 29 (5) (2008) 293–301. doi: 10.1007/s10072-008-0986-2.~~

[26] N.F. Abdelkader, M.M. Safar, H.A. Salem, Ursodeoxycholic acid ameliorates apoptotic cascade in the rotenone model of Parkinson's disease: modulation of mitochondrial perturbations, Mol. Neurobiol. 53 (2) (2016) 810-817. doi: 10.1007/s12035-014-9043-8.

[27] M.C. Bonferoni, L. Ferraro, B. Pavan, S. Beggiato, E. Cavalieri, P. Giunchedi, A. Dalpiaz, 2019. Uptake in the central nervous system of geraniol oil encapsulated in chitosan oleate following nasal and oral administration, Pharmaceutics. 11, 3. doi: 10.3390/pharmaceutics11030106.

[28] A. Dalpiaz, M. Fogagnolo, L. Ferraro, A. Capuzzo, B. Pavan, G. Rassu, A. Salis, P. Giunchedi, E. Gavini, Nasal chitosan microparticles target a zidovudine prodrug to brain HIV sanctuaries, Antiviral Res. 123 (2015) 146-157. doi: 10.1016/j.antiviral.2015.09.013.

[29] L. Casettari, L. Illum, Chitosan in nasal delivery systems for therapeutic drugs, J. Control. Release 190 (2014) 189–200. doi: 10.1016/j.jconrel.2014.05.003.

[30] L.R. Hanson, W.H. Frey 2nd. Strategies for intranasal delivery of therapeutics for the prevention and treatment of neuroAIDS, J. Neuroimmune Pharmacol. 2 (1) (2007) 81–86. doi: 10.1007/s11481-006-9039-x.

[31] M.C. Zink, Translational research models and novel adjunctive therapies for neuroAIDS, J. Neuroim. Pharmacol. 2 (1) (2007) 14–19. doi: 10.1007/s11481-006-9062-y.

[32] L. De Fazio, E. Spisni, E. Cavazza, A. Strillacci, M. Candela, M. Centanni, C. Ricci, F. Rizzello, M. Campieri, M.C, Valerii, 2016. Dietary geraniol by oral or enema administration strongly reduces dysbiosis and systemic inflammation in dextran sulfate sodium treated mice, Front. Pharmacol. 7, 38. doi: 10.3389/fphar.2016.00038.

[33] A.V. Turina, M.V. Nolan, J.A. Zygadlo, M.A. Perillo, Natural terpenes: Self-assembly and membrane partitioning, Biophys. Chem. 122 (2) (2006) 101–113. doi: 10.1016/j.bpc.2006.02.007.

[34] Aburahma, M. H., & Badr-Eldin, S. M. Compritol 888 ATO: a multifunctional lipid excipient in drug delivery systems and nanopharmaceuticals, Exp. Opin. on Drug Del. 11 (12) (2014) 1865–1883. doi: 10.1517/17425247.2014.935335.

[35] M.J. Gomes, C. Fernandes, S. Martins, F. Borges, B. Sarmento, Tailoring lipid and polymeric nanoparticles as siRNA carriers towards the blood-brain barrier - from targeting to safe administration, J. Neuroimmune Pharmacol., 12 (1) (2017) 107-119. doi: 10.1007/s11481-016-9685-6.

[36] W. Abdelwahed, G. Degobert, S. Stainmesse, H. Fessi, Freeze-drying of nanoparticles: Formulation, process and storage considerations, Adv. Drug Del. Rev. 58 (15) (2006) 1688–1713. doi: 10.1016/j.addr.2006.09.017.

[37] B. Pavan, A. Dalpiaz, Prodrugs and endogenous transporters: are they suitable tools for drug targeting into the central nervous system? Curr Pharm Des. 17 (32): (2011) 3560-3576.. doi: 10.2174/138161211798194486.

[38] B. Pavan, G. Paganetto, D. Rossi, A. Dalpiaz, Multidrug resistance in cancer or inefficacy of neuroactive agents: innovative strategies to inhibit or circumvent the active efflux transporters selectively, Drug Discov. Today. 19 (10) (2014) 1563-1571. doi: 10.1016/j.drudis.2014.06.004.

[39] Y. Jin, L. Xing, Y. Tian, M. Li, C. Gao, L. Du, J. Dong, H. Chen, Self-assembled drug delivery systems. Part 4. In vitro/in vivo studies of the self-assemblies of cholesteryl-phosphonyl zidovudine, Int. J. Pharm. 381 (1) (2009) 40−48. doi: 10.1016/j.ijpharm.2009.07.024.

[40] A. Dalpiaz, B. Cacciari, M. Mezzena, M. Strada, S. Scalia, Solid lipid microparticles for the stability enhancement of a dopamine prodrug, J. Pharm. Sci. 99 (11) (2010) 4730-4737. doi: 10.1002/jps.22178.

[41] A. Dalpiaz, M. Fogagnolo, L. Ferraro, S. Beggiato, M. Hanuskova, E. Maretti, F. Sacchetti, E. Leo, B. Pavan, Bile salt-coating modulates the macrophage uptake of nanocores constituted by a zidovudine prodrug and enhances its nose-to-brain delivery, Eur. J. Pharm. Biopharm. 144 (2019) 91-100. doi: 10.1016/j.ejpb.2019.09.008

[42] Y. Yang, H. Aloysius, D. Inoyama, Y. Chen, L. Hu, Enzyme-mediated hydrolytic activation of prodrugs, Acta Pharm. Sin. B 1 (3) (2011) 143–159. doi:10.1016/j.apsb.2011.08.001.

[43] S. Tang, A. Wang, X. Yan, L. Chu, X. Yang, Y. Song, K. Sun, X. Yu, R. Liu, Z. Wu, P. Xue, Brain-targeted intranasal delivery of dopamine with borneol and lactoferrin co-modified nanoparticles for treating Parkinson's disease, Drug Deliv. 26 (1) (2019) 700-707. doi: 10.1080/10717544. 2019.1636420.

[44] T. Musumeci, R. Pellitteri, M. Spatuzza, G. Puglisi, Nose-to-brain delivery: Evaluation of polymeric nanoparticles on olfactory ensheathing cells uptake, J. Pharm. Sci. 103 (2) (2014), 628–635. doi: 10.1002/jps.23836.

[45] O. Gartziandia, S.P. Egusquiaguirre, J. Bianco, J.L. Pedraz, M. Igartua, R.M. Hernandez, V. Préat, A. Beloqui, Nanoparticle transport across in vitro olfactory cell monolayer, Int. J. Pharm. 499 (1-2) 81–89 (2016). doi: 10.1016/j.ijpharm.2015.12.046.

[46] Y.M. Gabal, A.O. Kamel, O.A. Sammour, A.H. Elshafeey, Effect of surface charge on the brain delivery of nanostructured lipid carriers in situ gels via the nasal route. Int. J. Pharm. 473 (1-2) (2014) 442–457. doi: 10.1016/j.ijpharm.2014.07.025.

[47] J.M. Barichello, M. Morishita, K. Takayama, T. Nagai, Encapsulation of hydrophilic and lipophilic drugs in PLGA nanoparticles by the nanoprecipitation method, Drug Dev. Ind. Pharm. 25 (4) (1999) 471–476. doi: 10.1081/ddc-100102197.

[48] P. Ghasemiyeh, S. Mohammadi-Samani, Solid lipid nanoparticles and nanostructured lipid carriers as novel drug delivery systems: applications, advantages and disadvantages, Res. Pharm. Sci. 13 (4) (2018) 288-303. doi: 10.4103/1735-5362.235156.

[49] S. Kumar, N. Dilbaghi, R. Saharan, G. Bhanjana, nanotechnology as emerging tool for enhancing solubility of poorly water-soluble drugs, Bionanoscience 2 (4) (2012) 227–250. doi: 10.1007/s12668-012-0060-7.

[50] P. Kocbek, S. Baumgartner, J. Kristl, Preparation and evaluation of nanosuspensions for enhancing the dissolution of poorly soluble drugs, Int. J. Pharm. 312 (1-2) (2006) 179–186. doi: 10.1016/j.ijpharm.2006.01.008.

[51] A. zur Mühlen, C. Schwarz, W. Mehnert, Solid lipid nanoparticles (SLN) for controlled drug delivery – Drug release and release mechanism, Eur. J. Pharm. Biopharm. 45 (2) (1998) 149–155. doi: 10.1016/s0939-6411(97)00150-1.

[52] L. Djekic, J. Janković, A. Rašković, M. Primorac, Semisolid self-microemulsifying drug delivery systems (SMEDDSs): Effects on pharmacokinetics of acyclovir in rats, Eur. J. Pharm. Sci. 121 (2018) 287-292. doi: 10.1016/j.ejps.2018.06.005.

[53] Y. Jin, L. Yu, F. Xu, J. Zhou, B. Xiong, Y. Tang, X. Li, L. Liu, W. Jin, 2019. Pharmacokinetics of Active Ingredients of Salvia miltiorrhiza and Carthamus tinctorius in Compatibility in Normal and Cerebral Ischemia Rats: A Comparative Study, Eur. J. Drug Metab. Pharmacokinet., Dec 11. doi: 10.1007/s13318-019-00597-1.